2006

Observations of Triboelectric Charging Effects on Langmuir-Type Probes in Dusty Plasma

Aroh Barjatya
Utah State University, barjatya@erau.edu

Charles M. Swenson
Utah State University

Scholarly Commons Citation

Barjatya, A., and C. M. Swenson (2006), Observations of triboelectric charging effects on Langmuir-type probes in dusty plasma, J. Geophys. Res., 111, A10302, doi:10.1029/2006JA011806

Observations of triboelectric charging effects on Langmuir-type probes in dusty plasma

Aroh Barjatya[1] and Charles M. Swenson[1]

Received 20 April 2006; revised 2 June 2006; accepted 3 July 2006; published 5 October 2006.

[1] Investigation of Earth's mesosphere using sounding rockets equipped with a myriad of instruments has been a highly active field in the last 2 decades. This paper presents data from three separate instruments: an RF impedance probe, a DC fixed bias Langmuir probe, and an electric field probe, that were flown on a mesospheric sounding rocket flight investigating the presence of charged dust within and/or around a sporadic metal layer. The combined data set indicates a case of payload surface charging, the causes of which are investigated within this paper. A generic circuit model is developed to analyze payload charging and behavior of Langmuir-type instruments. The application of this model to the rocket payload indicates that the anomalous charging event was an outcome of triboelectrification of the payload surface from neutral dust particles present in the Earth's mesosphere. These results suggest caution in interpreting observations from the Langmuir class of instrumentation within dusty environments.

Citation: Barjatya, A., and C. M. Swenson (2006), Observations of triboelectric charging effects on Langmuir-type probes in dusty plasma, *J. Geophys. Res.*, *111*, A10302, doi:10.1029/2006JA011806.

1. Introduction

[2] Earth's mesosphere is a site of many phenomena associated with dust and aerosols such as sporadic atom layers, polar mesospheric summer echoes, and noctilucent clouds. Over the last few decades, these phenomena have been studied via modeling theory and remote observations, as well as in situ investigation using sounding rockets. One of the most important and ubiquitously used instruments for in situ investigation of electron density and temperature is the Langmuir-type probe, where a DC current is monitored from a voltage biased surface. This class of instrumentation is known to be sensitive to vehicle floating potential, ratio of payload surface area to probe surface area, and contamination of the probe surface, among other things [*Brace*, 1998, and references therein]. With all of their shortcomings, it is important that the data from this class of instrumentation be scrutinized for instrument and payload charging effects, so as to separate them from effects due to the phenomena under study.

[3] The 80–100 km mesospheric altitude range presents a different surface charging environment than the one present at satellite orbital altitudes, which have been extensively studied [*Garrett and Whittlesey*, 2000; *Hastings and Garrett*, 1996]. One difference is manifested by the enormous amount of meteoric ablation that condenses into dust particles and is suspended in the Earth's mesosphere between 80 and 100 km. The presence of dust at such a low altitude where the Debye length is greater than the average distance between dust particles constitutes a "dusty plasma," as compared to the "dust in plasma" at higher satellite orbital altitudes [*Shukla and Mamun*, 2002]. Charging of metallic surfaces by charge transfer from dust particles due to the difference in work functions or due to frictional contact is known as triboelectric charging. Although this is known to commonly occur under various conditions in the neutral planetary atmosphere, it has not been reported to date as one of the mechanisms for spacecraft charging. Within this paper we present evidence for a triboelectric charging event as a sounding rocket payload passed through a mesospheric dusty plasma.

[4] We first give an overview of the NASA Sudden Atom Layer sounding rocket payload, followed by the instrument description and data analysis of three of the onboard instruments: a radio frequency Swept Impedance Probe (SIP) for electron density measurement, a fixed bias (DC) Langmuir Probe (DCP) for relative electron density measurements, and a floating potential probe (V1S) that observed the voltage difference between the payload skin and a deployed floating sphere. We present an anomaly in the DCP and the V1S data set that points to a case of strong and sudden payload surface charging coincident with the mesospheric dust. We then develop a simple circuit model for spacecraft surface charging and Langmuir-type electric probe analysis. This model is subsequently applied to the SAL data and we conclude with a discussion of the surface charging event and its implications regarding probe behavior and the mesospheric neutral dust environment.

2. Sudden Atom Layer Investigation

[5] The NASA Sudden Atom Layer (SAL) sounding rocket (21.117) was launched as a part of the COQUI II

[1]Department of Electrical and Computer Engineering, Utah State University, Logan, Utah, USA.

0148-0227/06/2006JA011806

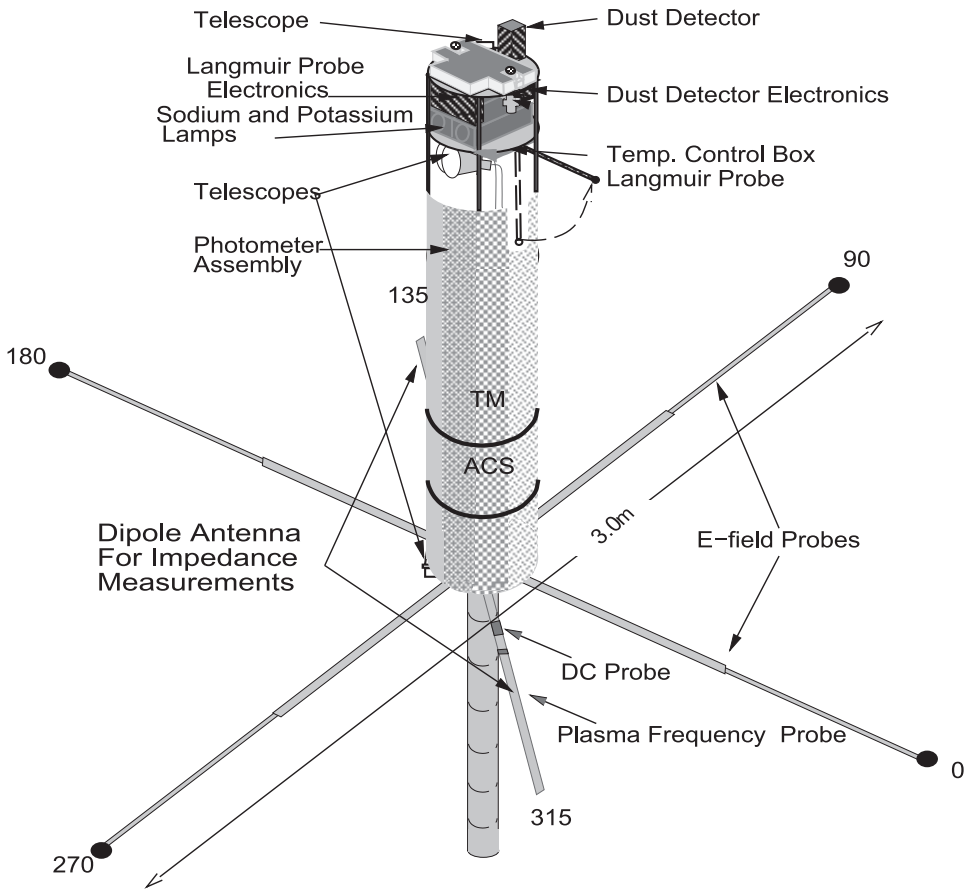

Figure 1. The Sudden Atom Layer (SAL) payload.

campaign from Puerto Rico on 19 February 1998 at 2009 LT. The rocket's main scientific purpose was the probing of sporadic sodium layers (Na_s). These are thin (1 km) layers of neutral atomic metal that form in the mesosphere (as observed by lidar), roughly within an altitude range of 90–100 km [*von Zahn et al.*, 1987]. Besides the three instruments whose data are the subject of this paper, the payload also included a charged dust detector, a Langmuir probe operating as Fast Temperature Probe to measure electron temperature, telescopes to measure sodium airglow, and photometers and lamps to measure neutral sodium density, the analysis of which have been published elsewhere [*Gelinas et al.*, 1998; *Hecht et al.*, 2000; *Kelley and Gelinas*, 2000]. Figure 1 depicts the payload instrument configuration.

[6] The payload reached a maximum altitude of 115.5 km and flew through two thin Na_s layers at 94 km and 97 km, with peak densities of 6000 cm^{-3} and 4000 cm^{-3}, as determined by the ground-based sodium lidar. Also, a sporadic E (E_s) layer at 92.5 km was detected by the Arecibo radar. The charged dust detector was mounted on the nose of the payload and an attitude control system was used to point the nose in the ram direction for the upleg, as well as the downleg, portion of the flight. It observed a 5 km thick, positively charged dust layer accompanying the lower Na_s layer. This data set is presented in Figures 2 and 3 within the paper by *Gelinas et al.* [1998]. The in situ photometer data has been presented in Figure 2 within the paper by *Hecht et al.* [2000].

2.1. Swept Impedance Probe (SIP)

[7] The impedance characteristics of an antenna immersed in an ionospheric plasma have been used to determine electron density for over 30 years [*Heikkila et al.*, 1968; *Balmain and Oksiutik*, 1969; *Baker et al.*, 1985; *Steigies et al.*, 2000]. The SIP consisted of two booms deployed 180 degrees apart with a 2-m tip-to-tip length and a 2.54 cm diameter. The instrument used the last 52.5 cm of the booms

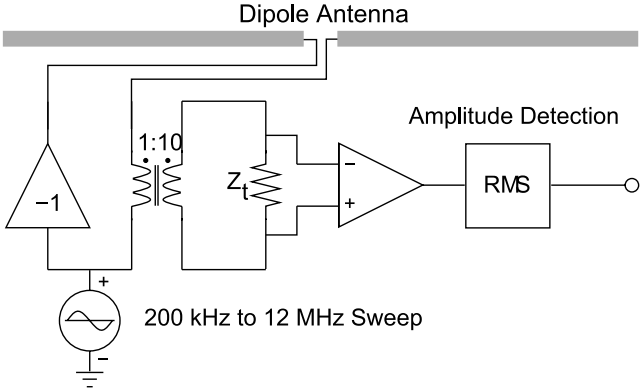

Figure 2. The SIP circuit.

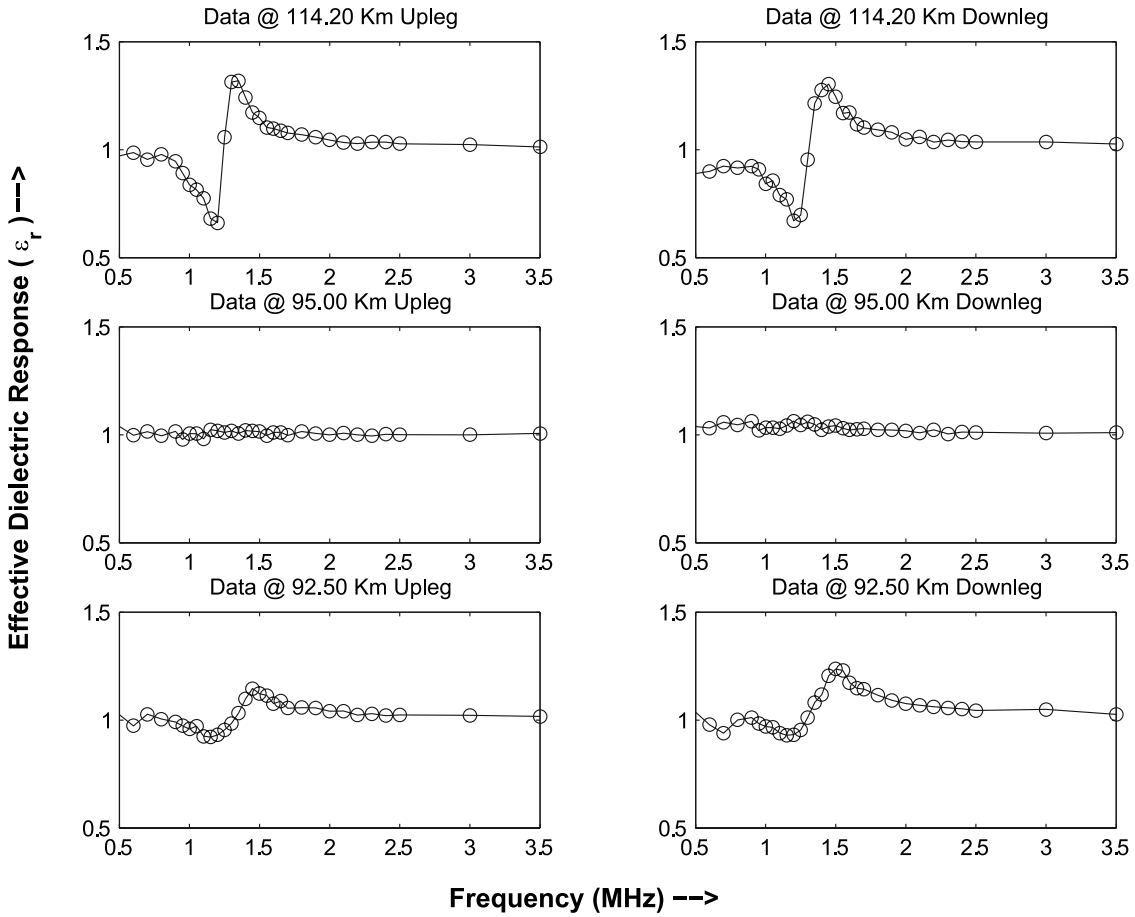

Figure 3. Effective dielectric response of the SIP antenna on the upleg and the downleg. Top and bottom panels show response of instrument within the E_s layer and the middle panel shows observations in low density plasma.

as active elements of the antenna. The antenna was differentially driven with a 1-Volt sinusoidal signal, with a frequency sweep at 40 fixed frequencies ranging over 0.2–12 MHz, at the rate of 96 sweeps per second. The magnitude of current flowing to the antenna was monitored using an RF current transformer as illustrated in Figure 2. Although the impedance probe was driven in a dipole configuration, the current was monitored on only one half of the antenna. The antenna was electrically short at the driving frequencies with a free space capacitance of C_0 = 2.6pf.

[8] The observed current magnitudes were converted to impedance magnitudes using preflight calibrations. We compute the effective dielectric response of the plasma surrounding the antenna, ϵ_r, as a function of frequency by

$$|\epsilon_r(f)| = \frac{Z_{plasma}(f)}{Z_0(f)} \tag{1}$$

where Z_0 is the observed magnitude of the free space antenna impedance and Z_{plasma} is the measured impedance magnitudes over the swept frequency range. Figure 3 shows the computed effective dielectric response for three different altitudes. The figure clearly shows that SAL flew through two distinct layers of high electron density, one at about 92.5 km and the other at 114.2 km. The center panel shows the low signal to noise ratio condition associated with low plasma density.

[9] In order to derive electron densities from this data, we compare the computed effective dielectric response to the theoretical effective dielectric response generated from Balmain's model for a monopole antenna in a cold collisional magnetized plasma [*Balmain*, 1964, 1969]. Balmain's model gives us the antenna impedance as a function of five parameters: the plasma frequency ω_p, the electron cyclotron frequency ω_c, the electron-neutral collision frequency ν_{en}, the angle with respect to magnetic field θ, and the ion sheath size S. We fit our data to Balmain's theory for frequencies above that of the upper hybrid resonance where the sheath resonances and the angle to magnetic field do not play an important role and are thus neglected. We used the IGRF (International Geomagnetic Reference Field) model to determine ω_c, which was found to be within 1% of 1.06 MHz during the entire flight. We also used electron momentum transfer collision frequencies [*Banks and Kockarts*, 1973; *Schunk and Nagy*, 2000] and neutral densities from the MSIS (Mass Spectrometer, Incoherent Scatter Radar Extended) model to find ν_{en} for the altitude profile of the rocket. The absolute electron density thus computed from the least squares fit to SIP data for ω_p is

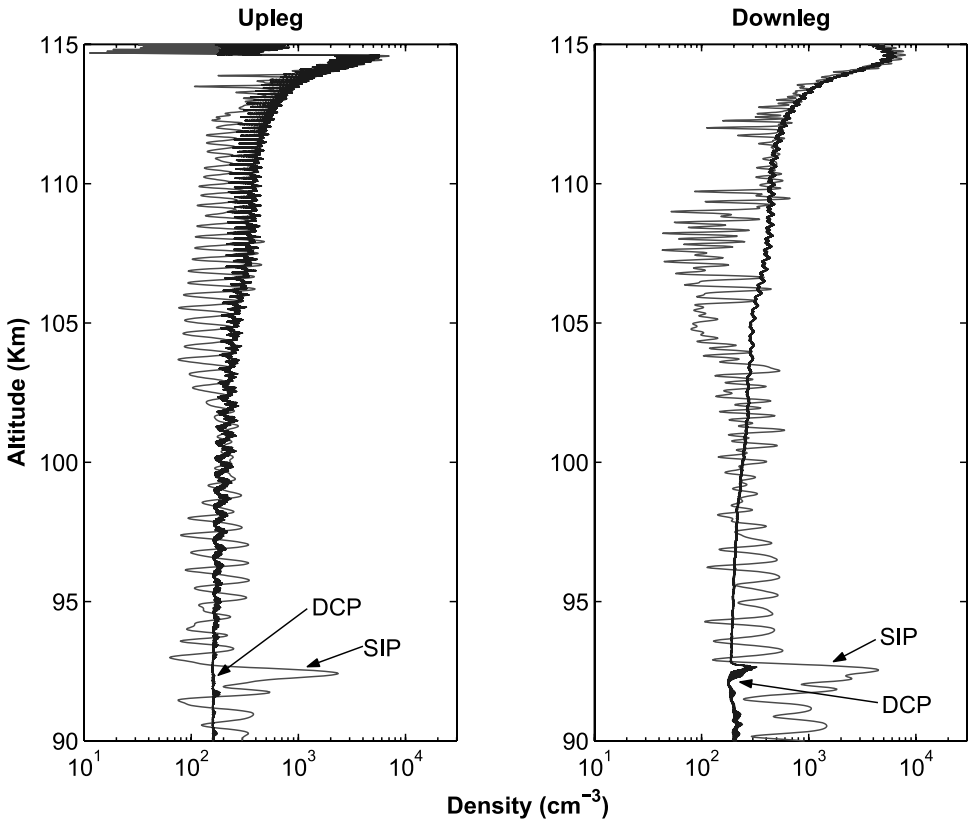

Figure 4. Comparison of density profiles from DCP and SIP. DCP data is normalized to SIP density at 114 km.

shown in Figure 4. The modulation in the derived electron density at the rocket spin rate is expected as the SIP antenna moved in and out of rocket wake at 1 Hz.

2.2. Fixed Bias Langmuir Probe (DCP)

[10] The DCP made use of two 5 cm long cylinders near the base of both the booms of dipole antenna (refer to Figure 1). As the instrument response was combined from two cylindrical probes deployed on booms that were 180 degrees apart, the spin modulation effect is thus subdued, but not eliminated. The probe was fixed bias +3 volts relative to the payload skin to measure the electron saturation current. The DCP relative density data, normalized to the SIP data at 114 km, is shown in Figure 4. The DCP was at its noise floor limit of 16×10^{-9} amperes in the lower-altitude range of 90–94 km. This current after normalization with SIP data corresponds to an electron density of about 150 cm^{-3}.

[11] The main theme of this paper is the investigation of the fact that the lower E_s layer observed by ground-based radar and also by the SIP is not present in the DCP data. We can be certain that this was not an instrument malfunction or failure, as the DCP did respond to the 114 km E_s layer and generally agrees well with the SIP data throughout the flight, especially if one takes into account a simulation of neutral wake effects to be discussed later.

2.3. V1S: Floating Potential Probe

[12] The E-field experiment on SAL used sets of 3 m tip-to-tip booms in the aft section of the payload to deploy four carbon-coated spheres of 7.62 cm diameter [*Gelinas*, 1999], as shown in Figure 1. Besides the E-field data the payload skin potential was monitored as a voltage difference between one of the spheres and the payload skin; this measurement is designated as V1S. The data is shown in Figure 5 as a function of rocket time of flight. The rocket passed through the 92.5 km E_s layer on the upleg at t = 103 s and on the downleg at t = 243 s. Within the layer an upward of 2 volt difference between the payload skin and sphere was observed. The E-field within the layer was on the order of 10 mV/m [*Gelinas*, 1999; *Kelley and Gelinas*, 2000] and thus does not account for the large potential seen in the V1S skin channel. Although the V1S measurement is not a direct observation of the payload floating potential, it is nevertheless an indicator of surface charging events that occur differentially between the sensor and payload along with the minor E-field effects.

3. Charging Circuit Model

[13] The typical assumption for spacecraft surface charging is that capacitive charging timescales are small compared to the timescales of interest and the process can be examined at steady state where all currents to the surface are balanced. The potential at which this balance occurs is called the floating potential when referenced to the ambient plasma environment, which is the reference point for all potentials in this paper. We have developed a nonlinear circuit model for a current collecting surface in a plasma and

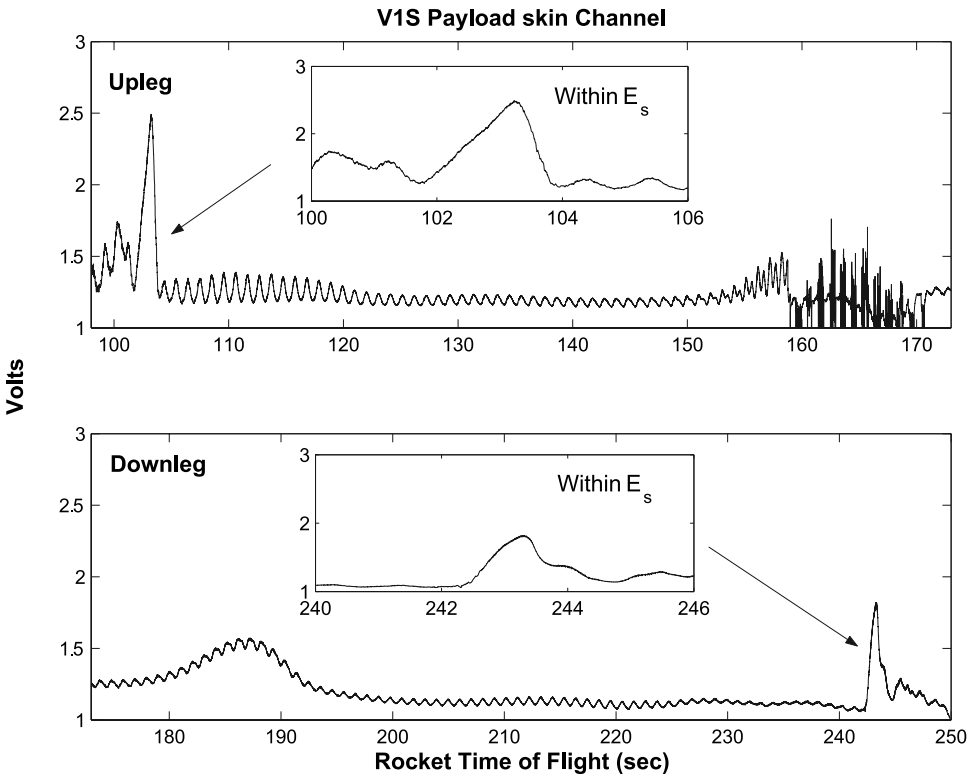

Figure 5. Upleg and downleg time of flight profiles of the floating potential probe (V1S).

implemented it in SPICE (Simulation Program with Integrated Circuit Emphasis), which is an industry standard simulation program used for simulating networks of linear and nonlinear circuit elements [*Keown*, 2001]. The numerical solvers available within SPICE are used to simultaneously calculate spacecraft floating potential and instrument response, including all the transient capacitive effects. We only consider the ion, electron, charged dust, and triboelectric currents in our model and neglect other plasma currents, since the payload was in darkness and in a low radiation environment.

[14] The E_s layer at 92.5 km is likely to have consisted of metallic ions like Fe^+ and Mg^+ [*Earle et al.*, 2000; *Roddy et al.*, 2004]. The Fe^+ ion thermal speed for T = 180 K (at 92.5 km) is about 285 m/s and the Mg^+ ion thermal speed is about 430 m/s. The rocket Earth relative speed at 92.5 km altitude was determined from the rocket trajectory to be 761 m/s on upleg and 744 m/s on downleg. As the rocket velocity is within a factor of 3 of these ion thermal velocities, we chose to model the ions as a thermal current to the first order, as justified by theory [*Hoegy and Wharton*, 1973; *Godard and Laframboise*, 1983].

[15] The ion and electron thermal currents (I_i, I_e) for a cylindrical collector are given by equation (2) and (3), where the subscript represents the charged species being modeled. The current due to electrons is modeled as positive current and the current due to ions is modeled as negative current. Equation (2) models the electron saturation and ion retardation region, whereas equation (3) models the electron retardation and ion saturation regions. For a spherical collector we remove the square-root from over the last term in the saturation current equation for both species.

$$\begin{aligned} I_e(V) &= Ane\sqrt{\frac{k_bT_e}{2\pi m_e}}\sqrt{\left(1+\frac{eV}{k_bT_e}\right)} \\ I_i(V) &= -Ane\sqrt{\frac{k_bT_e}{2\pi m_i}}\exp\left(\frac{-eV}{k_bT_e}\right) \end{aligned} \quad V > 0 \tag{2}$$

$$\begin{aligned} I_e(V) &= Ane\sqrt{\frac{k_bT_e}{2\pi m_e}}\exp\left(\frac{eV}{k_bT_e}\right) \\ I_i(V) &= -Ane\sqrt{\frac{k_bT_e}{2\pi m_i}}\sqrt{\left(1-\frac{eV}{k_bT_e}\right)} \end{aligned} \quad V \le 0 \tag{3}$$

where

A	surface area;
T_e	electron temperature;
n	plasma density;
V	surface potential;
e	elementary charge;
k_b	Boltzmann Constant;
m_e	electron mass;
m_i	ion mass.

[16] The above equations are for unmagnetized collisionless plasma. The presence of Earth's magnetic field and the collisional behavior of the plasma in mesosphere are ignored in order to keep the model simple and tractable [*Chen*, 1965], and their exclusion should not be a major limiting factor affecting the accuracy of the model.

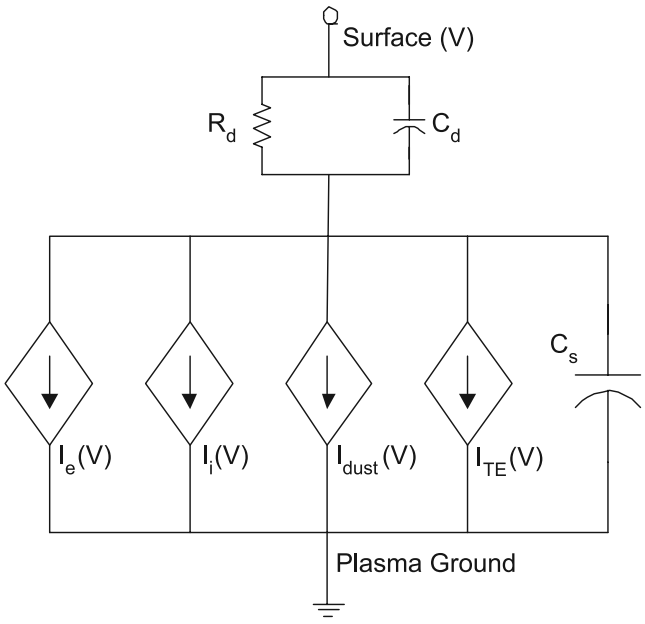

Figure 6. The SPICE voltage-controlled-current-source circuit model for payload and probe surfaces.

[17] The dust, being at least an order of magnitude heavier than ions, is relatively immobile and is modeled as a ram current (I_{dust}). The dust particle speed distribution is very narrow around the ram speed, and therefore the current drops as a unit step function, H, whenever the surface potential exceeds the directed ram energy. This relation is expressed by equation (4). As the dust observed in situ by SAL is positively charged, the current due to dust is modeled as negative current.

$$I_{dust}(V) = -A_{ram} e n_d V_{ram} H[\varepsilon - eV] \tag{4}$$

where

A_{ram} ram surface area;
e fundamental charge;
n_d dust charge density;
V_{ram} ram velocity;
ε $\frac{1}{2} m_{dust} V_{ram}^2$.

[18] We also model a fourth current source due to triboelectric charging (I_{TE}) from the neutral dust present in the Earth's mesosphere. Triboelectric charging refers to charge buildup or deficit that occurs when two different materials come under either simple or frictional contact. If two metals come merely in contact with each other and then separate, the metal surface with lower work function loses an electron to the surface with higher work function [*Harper*, 1967]. The type of charge transfer is entirely contact initiated and is not affected by the velocity of separation or by frictional sliding during separation [*Lowell*, 1975]. The payload skin was aluminium (ϕ_{wk} = 4.2 eV), and although the composition of dust was unobserved in situ, we assume the metallic composition of the dust to be similar to that in meteorites [*Plane*, 2004; *McNeil et al.*, 2002]. Thus the dust was most probably composed of potassium (ϕ_{wk} = 2.29 eV), sodium (ϕ_{wk} = 2.36 eV), calcium (ϕ_{wk} = 2.87 eV), magnesium (ϕ_{wk} = 3.66 eV), and iron (ϕ_{wk} = 4.67 eV). All oxidized metals behave, as far as contact charging is concerned, like a different metal with a work function equal to the depth of the acceptor levels in the adsorbed oxygen, which is about 5.5 eV and is largely independent of the nature of the metal [*Cabrera and Mott*, 1949; *Sternovsky et al.*, 2001]. The presence of atomic sodium, as observed by lidar, leads us to believe that there was a population of dust particles with unoxidized sodium or other low work function metal adsorbed on their surface. Thus the triboelectric charging current source in the circuit model will be sourcing positive current, as each unoxidized dust particle with work function lower than 5.5 eV will leave one electron on the oxidized aluminium payload skin. The triboelectric current is modeled by equation (5)

$$I_{TE}(V) = A_{ram} e N V_{ram} \tag{5}$$

where N is the component of neutral dust depositing the net triboelectric current.

[19] Each of the above current sources has been coded as a voltage-controlled-current-source (VCCS) and make up a single subcircuit model, as shown in Figure 6. We model the contamination present on a current collecting surface as a parallel combination of a capacitor C_d and resistor R_d [*Piel et al.*, 2001]. The sheath is modeled as another capacitance C_s in parallel with the current sources. The current equations, including capacitive effects, are solved by SPICE simultaneously to find the floating potential of the spacecraft. The payload is modeled as a cylinder with its nose cone and aft skirt ejected and a total length of 4 m and a diameter of 43 cm. The rocket was pointing to within 2° of the ram direction on the upleg and within 8° on the downleg. We meticulously calculate separate payload ram projected areas for the upleg and downleg case. Figure 7 shows the electrical circuit model of SAL in SPICE. Each current source shown is a complete subcircuit of Figure 6, incorporating four different current sources. The difference between the subcircuit model used for DCP and that used for the payload collecting surface is manifested by different collecting areas, which are passed to the subcircuit in a function call. We also model a spherical probe coated with carbon (ϕ_{wk} = 5 eV) for estimating the V1S channel.

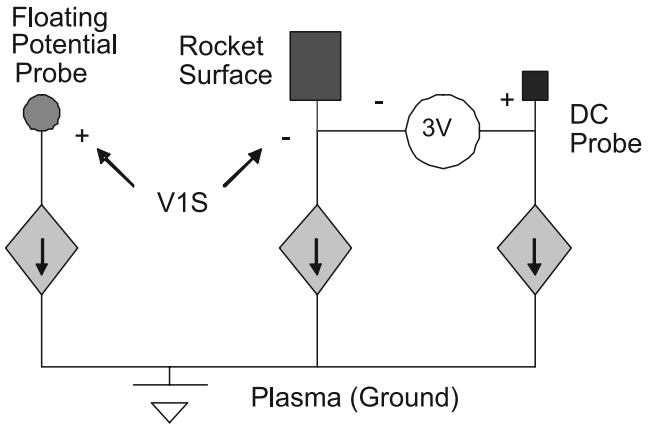

Figure 7. The circuit model of the SAL payload, DC Langmuir probe, and floating potential probe.

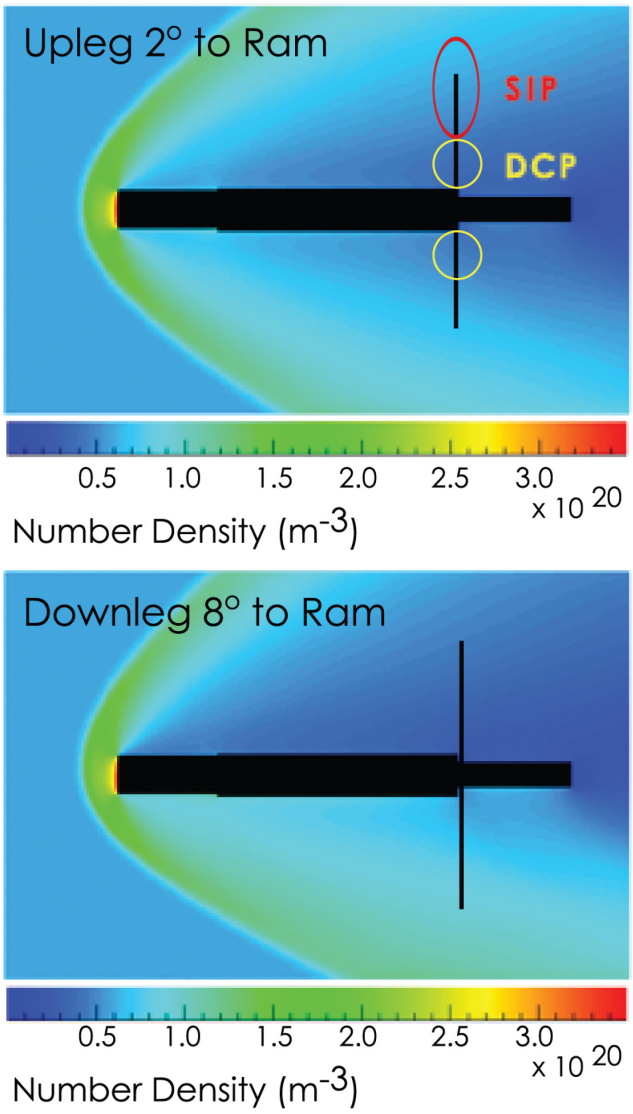

Figure 8. DSMC simulations of SAL payload wake on upleg and downleg.

[20] As a check for the model, we calculate the V1S observed potential outside the E_s layer using density as observed by the SIP. We represent the DCP and the payload skin with cylindrical surface current equations, and the floating potential probe with spherical surface equations. Using correct DCP to payload skin area ratio, V1S simulated magnitude is 1.37 volts, which agrees quite well with the V1S channel outside the lower E_s layer (see Figure 5).

4. Discussion

[21] The wake in the neutral atmosphere around a sounding rocket at mesospheric altitudes is well known and its perturbing effects on in situ observations must be considered. The neutral wake perturbs the plasma environment through strong collisional coupling such that data from radially mounted probes spinning through this wake show "spin modulation." The radial variation in the particle density thus affects magnitude of the electron density and other measurements. We computed this wake effect for neutral particle density through a 2-D Direct Simulation Monte Carlo (DSMC) numerical calculation [*Bird*, 1994]. The simulation was done for rocket flight conditions at 92.5 km altitude, where the total neutral number density and temperature are approximated from the MSIS model to be 5.93×10^{19} particles/m^3 and 180K, respectively. We simulated three neutral species, namely O_2, N_2, and Ar. We use the same payload dimensions as in the charging model and do two separate simulations for the different angles to the ram direction on upleg and downleg. The results are shown in Figure 8. Although the booms were not included in the simulation, they have been superimposed within the figure to show the position of SIP and DCP within the wake structure.

[22] Figure 8 shows that on the upleg the density around DCP will see a minimum reduction by a factor of 2 and the SIP should see a minimum reduction by a factor of 1.25 relative to the ambient plasma density. On the downleg, although the SIP monopole should see an enhanced density as it swings into and out of the ram side of the rocket, the DCP is averaging the signal from both the booms and should see less of a density swing. All of this corresponds well with data outside the 92.5 km E_s layer, as shown in Figure 4, where the SIP density swings up and below the DCP observed density. However, this does not explain the total absence of DCP response on the upleg and its low response on the downleg within the lower E_s layer.

[23] *Sternovsky et al.* [2004] have shown that the presence of charged aerosols in the mesosphere can lead to a charged rocket wake affecting E-field or floating probes. The characteristics of this charged wake are dependent on the polarity of the charge on the aerosols and the amount of charge residing on the aerosols. The DROPPS mission observed that all of the negative charge was on the heavy aerosols, which led to charge separation between the ions, embedded in the neutral flow, and the aerosols that are not affected by the flow. This created a strong potential structure within the wake, which was observed by the E-field instrument. The SAL payload saw a completely different situation, in which a relatively small amount of positively charged dust (20 particles/cm^3) was observed coincident with the lower E_s layer. Electrons, being lighter, are assumed to follow both the ions and the positively charged dust particles, with the only charge separation being that attributed to ambipolar diffusion. Thus, we do not expect a charged wake as was observed in DROPPS. This is consistent with the absence of spin modulation in V1S data. In a charged wake the potential structure around the payload is correlated to the plasma density; thus a spin modulation in V1S similar to the SIP data would have been consistent with a DROPPS like charged wake.

[24] The reduction in current collected by the DCP in the lower E_s layer must be due to negative charging of the payload, more than the 3 volts bias on the probe, so as to remove the DCP from operating in the electron saturation region. Figure 9 focuses on the 90–93 km altitude range and presents all three instrument data sets for correlation. Once again, spin modulated SIP density data is observed within the E_s, while the DCP completely misses this layer. The V1S data suggests payload charging in the region where the DCP did not respond, with a peak differential

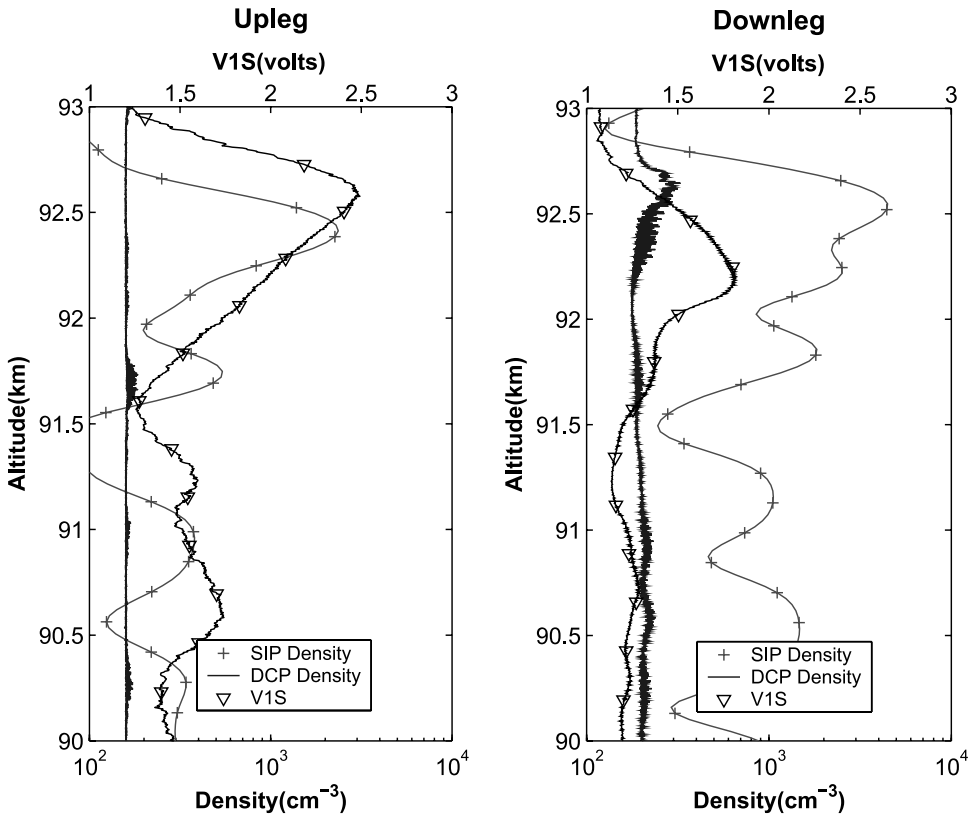

Figure 9. Profiles of SIP and DCP electron densities and V1S potential between 90 and 93 km.

charging at 2.5 volts on the upleg and 1.8 volts on the downleg. This observation, along with the indication by the DCP that the payload surface was more than 3 volts negative, indicates that both the carbon coated sensor and the payload surface experienced a negative charging event, with the payload surface charging more. The difference in their levels of charging could be due to differences in shape and surface work function.

[25] We used our circuit model to simulate the charging of the payload along with the DCP and V1S instrument responses. The plasma density at the location of the DCP and the floating sphere was estimated within the wake by scaling the SIP density with the results of the DSMC simulation. We started with the simplest model, considering only ions and electrons without capacitive contamination effects, charge dust, or triboelectric current sources. This basic simulation did not show any significant levels of payload charging in the lower E_s layer. On the other hand, modeling the ions as a pure ram current led to severe charging throughout the entire layer and did not produce the observed V1S data profile. The inclusion of various capacitance and resistance values to account for the contamination and sheath effects on the probe and payload surfaces also did not produce the observed DCP and V1S profiles. We approximated the positive charged dust density based on data from the charged dust detector and used it in the simulation. However, as the charged dust density was only 20 particles/cm^3, the effect of this charged dust current source was also not enough to produce the required DCP and V1S profiles. Thus we conclude that an additional triboelectric current source from neutral dust in the mesosphere is needed to explain the sudden payload charging within the 92.5 km layer.

[26] Estimating the density of neutral dust responsible for triboelectrification is problematic due to the lack of observations of the dust composition. One may assume that most of the metallic dust material encountered by the payload existed in an oxidized state and thus little triboelectric charging would be expected against the payload's oxidized aluminium surface due to similar work functions. Yet, both in situ and ground-based observations indicated the strong presence of atomic sodium. Sodium may have been adsorbed on the dust surface in its atomic form and could have been the reservoir for Na_s layer, as has been hypothesized elsewhere by *von Zahn et al.* [1987]. Such dust would supply an additional current due to work function differences. There is a possibility that other higher work function metals might have supplied an opposite current, but the net current required to produce the observed charging must have come from low work function metals. The triboelectric current density required to reproduce the DCP and V1S response is presented in Figure 10, along with the in situ observations of Sodium Volume Emission Rates [*Hecht et al.*, 2000]. We note that this current is located below the stronger Na_s signature and within the E_s layer observed by the SIP. This vertical separation of the atomic sodium from the neutral dust responsible for triboelectrification of the payload could be due to neutral winds or gravity waves and might also justify the separate life times of the E_s and Na_s layer [*von Zahn and Hansen*, 1988].

[27] The simulation results including triboelectric charging effects are shown in Figure 11. The factor used to

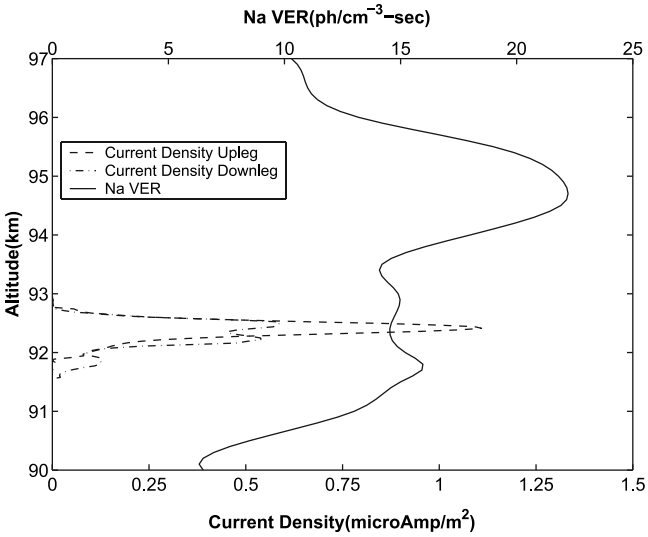

Figure 10. Required triboelectric current density along with in situ observed sodium volume emission rate (VER).

normalize the flight DCP data to the SIP density at 114 km was also used to normalize the charging model's DCP current. Furthermore, we also simulated a noise floor of 16×10^{-9} amperes that shows up as the instrument sensitivity floor at about 150 e/cm^3. The V1S data from the simulation is expected to be only an approximate match to the observed data throughout the entire 90–93 km altitude region due to spin phase wake differences in ambient density seen at the V1S sphere which was deployed in a different direction than the SIP. We did not model this temporal (and thus altitude) spin phase difference for the charging calculations of the V1S sphere.

[28] The simulation derived the additional current required to generate the observed DCP and V1S profile. If we simply correlate this triboelectric current as a single charge transfer from a solitary dust particle, then the required neutral dust layer has peak density that is on the order of several thousand particles/cm^3, which is on the same order as predicted by the Hunten model [*Hunten et al.*, 1980] for subnanometer mesospheric smoke particles between 90 and 95 km. Although the model is widely accepted, these neutral smoke particles have never been directly observed and measured in situ, and their density should vary with meteoric activity and neutral winds. What is surprising is that the triboelectrically reactive component of the dust was confined to an altitudinally narrow band. The neutral dust could well have existed over a much broader altitude range, as predicted by Hunten's model, but the compositional variation of the dust could have been responsible for the thin altitude feature that we observed. This thin triboelectrically reactive neutral dust layer was within the broader (5 km) charged dust layer observed by the charged dust detector. This in turn implies that for some reason there was a higher concentration of adsorbed sodium or other low work function metal on the neutral dust, right where the E_s layer existed. The difference in the layer density and altitude spread between upleg and downleg is

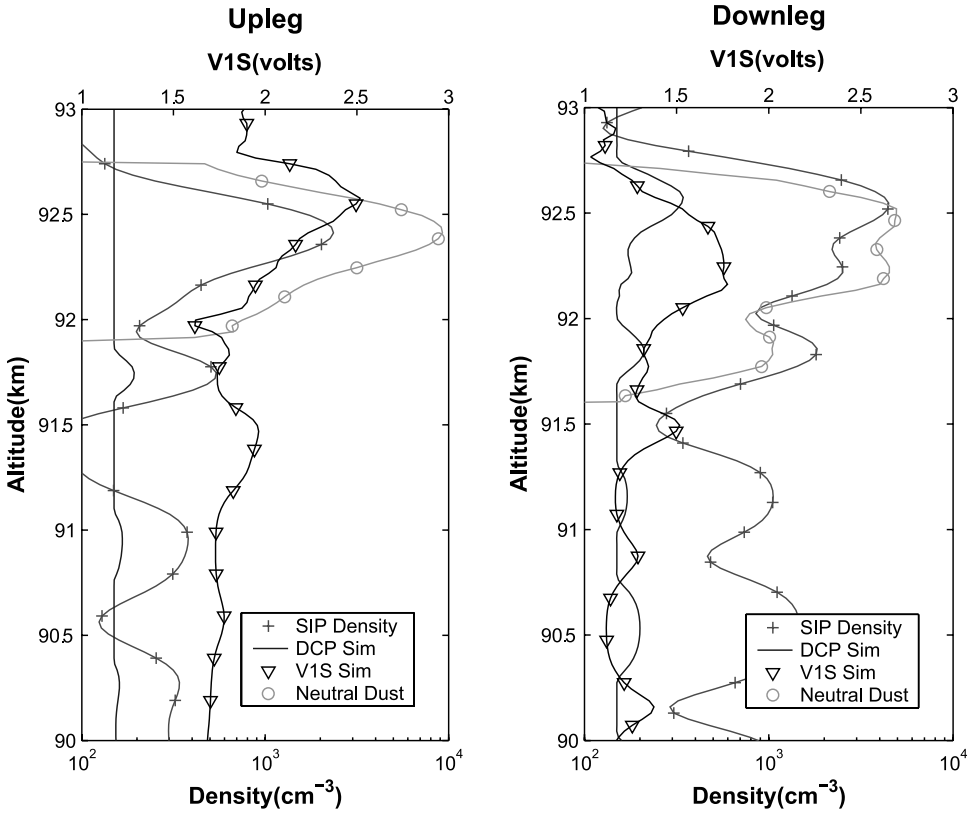

Figure 11. Charging model simulation response of DCP and V1S along with effective neutral dust density producing triboelectric charging.

possible as there was a horizontal distance of about 50 km between the two legs of the flight trajectory as the payload passed through the lower E_s layer. The absence of triboelectric charging of the payload within the 114 km layer was likely due to little or no neutral dust presence at that high an altitude, which is corroborated by the fact that no charged dust was observed around that layer.

[29] One might ask whether or not this phenomenon has been observed before. At this point it is important to note again that contact electrification is an unpredictable process that is hard to precisely replicate even in laboratory conditions [*Harper*, 1967; *Sternovsky et al.*, 2001]. Thus depending on the ambient neutral dust density, the major metallic composition of the neutral dust particles, and the difference between the major neutral dust constituent and the payload surface metal one could expect varying positive or negative charging results. Triboelectrification may have occurred on four recent sounding rocket flights from Poker Flat, Alaska, the results of which have been published earlier by *Gelinas et al.* [2005]. Although these flights were flown into layers of metallic composition, the layers were not sporadic atom layers. Within these metallic layers, the sodium density was about a factor of 4 lower than the iron density [see *Gelinas et al.*, 2005, Figure 5]. If we are to assume that both of these metal layers had mesospheric dust as their source, then iron should have been the major constituent of the neutral dust on that night. Considering simply the work functions of aluminium ($\phi_{wk} = 4.2$ eV) and iron ($\phi_{wk} = 4.67$ eV), it is possible that the sudden bumps in the electron density profiles were generated by triboelectric charging of the payload and the charging would be in the opposite direction to what was observed on SAL flights. This shift of payload potential would have put the fixed bias Langmuir probe further in electron saturation region, thus increasing the current observed.

[30] Another significant implication of our analysis is that if the DCP on SAL payload had been more sensitive and observed currents down to 1×10^{-11} amperes, we might have seen a "bite-out" in the electron density profile, even though the SIP and ground based data sets showed a sporadic E layer. Arguing that these layers are patchy by nature, one cannot compare in situ observations with ground-based observations, unless they were made over common volume. Thus it is important to fly a fairly high-resolution absolute electron density probe, such as the SIP, in order to correctly interpret the high resolution relative density profile from Langmuir-type probes.

5. Summary and Conclusion

[31] In this paper we have presented data from an RF impedance probe, a fixed bias DC Langmuir probe, and a payload skin floating potential measurement on a sounding rocket flight investigating mesospheric sudden atom layers. We have used Balmain's theory for antenna in cold magnetoplasma to derive absolute electron density from the RF impedance probe data and subsequently used those to calibrate the fixed bias DC Langmuir probe to derive high-resolution relative electron density. The coupled observations made by the three instruments presented in this paper imply very interesting payload charging dynamics that lead to anomalous DCP behavior. We have then developed and presented a charging circuit model and applied it to the sounding rocket payload. After investigating various reasons for the anomalous DCP behavior, including a detailed study of the neutral wake, we have concluded that the triboelectrification of the payload surface from mesospheric neutral dust was the reason for the anomalous DCP response.

[32] Besides the SAL data set, we have also discussed the phenomenon of triboelectrification of payload surface for another mesospheric sounding rocket campaign. Both of these data sets clearly indicate the importance for considering the effects of triboelectrification on the interpretation of Langmuir-type probe data sets in presence of dusty plasma. The circuit model simulation derived neutral dust density layer has a peak density that corresponds well with the existing theory. It is thus possible that triboelectrification effects may also be used as an instrumentation technique for observing the neutral dust composition, as well as neutral dust density.

[33] **Acknowledgment.** Amitava Bhattacharjee thanks Edward Thomas Jr. and Wayne A. Sales for their assistance in evaluating this paper.

References

Baker, K., J. Labelle, R. Pfaff, L. Howlett, N. Rao, J. Ulwick, and M. Kelly (1985), Absolute electron density measurements in the equatorial ionosphere, *J. Atmos. Terr. Phys.*, *47*, 781.

Balmain, K. (1964), The impedance of a short dipole antenna in a magnetoplasma, *IEEE Trans. Antennas Propagat.*, *AP-12*, 605.

Balmain, K. (1969), Dipole admittance for magnetoplasma diagnostics, *IEEE Trans. Antennas Propagat.*, *AP-17*, 389.

Balmain, K., and G. Oksiutik (1969), Rf probe admittance in the ionosphere: Theory and experiment, in *Plasma Waves in Space and in the Laboratory*, vol. 1, edited by J. Thomas and B. Landmark, p. 247, Elsevier, New York.

Banks, P., and G. Kockarts (1973), *Aeronomy, Part A*, Elsevier, New York.

Bird, G. A. (1994), *Molecular Dynamics and the Direct Simulation of Gas Flows*, Oxford Univ. Press, New York.

Brace, L. H. (1998), Langmuir probe measurements in the ionosphere, in *Measurement Techniques in Space Plasmas: Particles*, *Geophys. Monogr. Ser.*, vol. 102, edited by R. E. Pfaff et al., p. 23, AGU, Washington, D. C.

Cabrera, N., and N. Mott (1949), Theory of the oxidation of metals, *Rep. Prog. Phys.*, *12*, 163.

Chen, F. (1965), Electric probes, in *Plasma Diagnostic Techniques*, edited by R. Huddlestone and S. Leonard, p. 113, Elsevier, New York.

Earle, G. D., T. J. Kane, R. F. Pfaff, and S. R. Bounds (2000), Ion layer separation and equilibrium zonal winds in midlatitude sporadic e, *Geophys. Res. Lett.*, *27*(4), 461.

Garrett, H., and A. Whittlesey (2000), Spacecraft charging, An update, *IEEE Trans. Plasma Sci.*, *28*(6), 2017.

Gelinas, L. (1999), An in-situ measurement of charged mesospheric dust during a sporadic atom layer event, Ph.D. thesis, Univ. of N. H., Durham.

Gelinas, L., K. Lynch, M. Kelley, S. Collins, S. Baker, Q. Zhou, and J. S. Friedman (1998), First observation of meteoric charged dust in the tropical mesosphere, *Geophys. Res. Lett.*, *25*(21), 4047.

Gelinas, L., K. Lynch, M. Kelley, R. Collins, M. Widholm, E. MacDonald, J. Ulwick, and P. Mace (2005), Mesospheric charged dust layer: Implications for neutral chemistry, *J. Geophys. Res.*, *110*, A01310, doi:10.1029/2004JA010503.

Godard, R., and J. Laframboise (1983), Total current to cylindrical collectors in collisionless plasma flow, *Planet. Space Sci.*, *31*(3), 275.

Harper, W. R. (1967), *Contact And Frictional Electrification*, Oxford Univ. Press, New York.

Hastings, D., and H. Garrett (1996), *Spacecraft-Environment Interactions*, Cambridge Univ. Press, New York.

Hecht, J. H., S. Collins, C. Kruschwitz, M. C. Kelly, R. G. Roble, and R. L. Walterscheid (2000), The excitation of the na airglow from coqui dos rocket and ground based observations, *Geophys. Res. Lett.*, *27*(4), 453.

Heikkila, W., N. Eaker, J. Fejer, and K. Tipple (1968), Comparison of several probe techniques for ionospheric electron concentration measurements, *J. Geophys. Res.*, *73*(11), 3511.

Hoegy, W., and L. Wharton (1973), Current to a moving cylindrical electrostatic probe, *J. Appl. Phys.*, *44*(12), 5365.

Hunten, D., R. Turco, and O. Toon (1980), Smoke and dust particles of meteoric origin in the mesosphere and stratosphere, *J. Atmos. Sci.*, *37*, 1342.

Kelley, M., and L. Gelinas (2000), Gradient drift instability in midlatitude sporadic e layers: Localization of physical and wavenumber space, *Geophys. Res. Lett.*, *27*(24), 457.

Keown, J. (2001), *OrCAD PSpice and Circuit Analysis*, 4th ed., Prentice-Hall, Upper Saddle River, N. J.

Lowell, J. (1975), Contact electrification of metals, *J. Phys. D Appl. Phys.*, *8*, 53.

McNeil, W., E. Murad, and J. Plane (2002), Models of meteoric metals in the atmosphere, in *Meteors in the Earth's Atmosphere*, edited by E. Murad and I. Williams, p. 265, Cambridge Univ. Press, New York.

Piel, A., M. Hirt, and C. T. Steigies (2001), Plasma diagnostics with Langmuir probes in the equatorial ionosphere: I. the influence of surface contamination, *J. Phys. D Appl. Phys.*, *34*, 2643.

Plane, J. (2004), A new time-resolved model of the mesospheric na layer: Constraints on the meteor input function, *Atmos. Chem. Phys. Discuss.*, *4*, 39.

Roddy, P. A., G. D. Earle, C. M. Swenson, C. G. Carlson, and T. W. Bullett (2004), Relative concentrations of molecular and metallic ions in mid-latitude intermediate and sporadic-e layers, *Geophys. Res. Lett.*, *31*, L19807, doi:10.1029/2004GL020604.

Schunk, R. W., and A. F. Nagy (2000), *Ionospheres-Physics, Plasma Physics, and Chemistry*, Cambridge Univ. Press, New York.

Shukla, P., and A. Mamun (2002), *Introduction to Dusty Plasma Physics*, Inst. of Phys., Philadelphia, Pa.

Steigies, C. T., D. Block, M. Hirt, B. Hipp, A. Piel, and J. Grygorczuk (2000), Development of a fast impedance probe for absolute electron density measurements in the ionosphere, *J. Phys. D Appl. Phys.*, *33*, 405.

Sternovsky, Z., M. Horanyi, and S. Robertson (2001), Charging of dust particles on surfaces, *J. Vac. Sci. Technol.*, *19*(5), 2533.

Sternovsky, Z., R. Holzworth, M. Horanyi, and S. Robertson (2004), Potential distribution around sounding rockets in mesospheric layers with charged aerosol particles, *Geophys. Res. Lett.*, *31*, L22101, doi:10.1029/2004GL020949.

von Zahn, U., and T. Hansen (1988), Sudden neutral sodium layers: A strong link to sporadic e layers, *J. Atmos. Terr. Phys.*, *50*, 93.

von Zahn, U., P. von der Gathen, and G. Hansen (1987), Forced release of sodium from upper atmospheric dust particles, *Geophys. Res. Lett.*, *14*, 76.

A. Barjatya and C. M. Swenson, Department of Electrical and Computer Engineering, Utah State University, 4200 Old Main Hill, Logan, UT 84322, USA. (arohb@cc.usu.edu; charles.swenson@usu.edu)